Article ID: 1006-8775(2017) 01-0103-10

NUMERICAL SIMULATION OF INFLUENCE OF STRATOSPHERIC METHANE ON TROPICAL WATER VAPOR AND TEMPERATURE

WANG Shu-chang (王舒畅), ZHAO Jun (赵 军), WU Jian-ping (吴建平), CAO Xiao-qun (曹小群)
(Academy of Ocean Science and Engineering, National University of Defense Technology, Changsha 410073 China)

Abstract: Climatic characteristics of tropical stratospheric methane have been well researched using various satellite data, and numerical simulations have furtherly conducted using chemical climatic models, while the impact of tropical stratospheric methane oxidation on tropical distribution of water vapor is not paid enough attention in general circulation models. Parameterization of methane oxidation is taken into account to deal with the chemical moisturizing action due to the methane oxidation in this paper. Numerical simulation and analysis of the influence of stratospheric methane on the prediction of tropical stratospheric moisture and temperature fields using general circulation model is conducted using heavy storm cases including a heavy rain in South China and a typhoon caused tropical storm. The results show obvious impact of methane oxidation on the forecasting precipitation. It is demonstrated that the stratospheric water vapor in the tropic is significantly remedied by introducing of parameterization of methane oxidation. And prediction of stratospheric temperature is accordingly modified, especially in the lower stratosphere within 30°N. The verification of monthly mean of forecast anomaly correlation (ACC) and root mean square (RMS) errors over the tropics indicated that the impact of stratospheric methane is neutral as to the forecast of geopotential height, and positive to the forecast of temperature and winds over the tropics.

Key words: methane oxidation; Parameterization; tropical stratosphere; water vapor
CLC number: P421 **Document code:** A
doi: 10.16555/j.1006-8775.2017.01.010

1 INTRODUCTION

Methane is a powerful greenhouse gas produced by natural and anthropogenic sources at the earth's surface. Combined with the fact that the percentage rate of concentration increase of methane is significantly greater than that of carbon dioxide, one can argue that the role of methane in greenhouse gas accumulation appears to be comparable with carbon dioxide. Currently, volume mixing ratio of methane is around 1.7 ppmv. It is carried upwards in the tropical stratosphere and decreases in relative density (due to oxidation) to values of around 0.2–0.4 ppmv around the stratopause.

The methane data observed by HALOE in UARS satellite are widely used to analyze the temporal and spatial features of stratospheric methane. The features of distribution and seasonal variations of stratospheric CH_4 mixing ratio over China is analyzed using the methane data from HALOE experiment on UARS[1]. Then Bi et al.[2] used the HALOE observational data to analyze the vertical and horizontal distributions of H_2O and CH_4 in the middle atmosphere, especially in the upper stratosphere and mesosphere. Guo et al.[3] analyzed the temporal and spatial features of stratospheric methane and its relation to ozone variation using the methane data observed by HALOE in UARS satellite. Zheng and Shi[4] studied the influence of the residual currents induced by QBO on the CH_4 double peaks by analyzing the CH_4 data from HALOE. The formation mechanism of the methane QBO in the extra-tropics was examined through a set of ideal comparative experiments with and without the wind QBO by BI et al. [5].

It is known that the tropospheric increase in CH_4 mixing ratios, which is well documented (Blake and Rowland[6]; Dlugokencky et al.[7]), has contributed to, but cannot entirely explain the observed increase in stratospheric water vapour (Engel et al.[8]). A study of stratospheric humidity in analyses and multi-year simulations has shown that a broadly realistic distribution of water vapour at, and immediately above the tropopause, and that the slow upward transfer of water vapour in the tropical stratosphere could be captured quite reasonably given sufficiently fine vertical resolution in the model [9]. However, values of water vapour in the tropical upper stratosphere, and throughout much of the extratropical stratosphere, were too low. Something must be done to remedy this deficiency in order to producing realistic stratospheric water vapor using a general circulation model including the whole stratosphere. Introduction of a simple parametrization of the upper-stratospheric moisture source due to methane oxidation and a sink due to

Received 2015-03-11; **Revised** 2017-01-25; **Accepted** 2017-02-15
Foundation item: National Basic Research Program of China (2013AA7033039E); National Natural Science Foundation of China (41475094)
Biography: WANG Shu-chang, Ph.D., primarily undertaking study on medium-range numerical weather prediction.
Corresponding author: WANG Shu-chang, e-mail: wangshuchang@126.com

photolysis in the mesosphere would be conducted and tested in this paper.

This paper is organized as follows. After introducing the climatic character of methane and water vapor in stratosphere outlined in section 1, basic principles and formulations of parameterization of methane oxidation are described briefly in section 2. The experimental configuration and two heavy rain cases chosen to demonstrate how the methane oxidation impacts the humidity and temperature forecasting of the general circulation model is presented in section 3. In section 4, several measures of the efficacy of the methane oxidation parameterization scheme in perfecting the most real temperature, humidity and precipitation of the model results were investigated. Conclusions and discusses are made finally.

2 BASIC PRINCIPLES AND FORMULATIONS

2.1 *Methane oxidation parameterization*

Molecular hydrogen (H_2), methane (CH_4) and water vapor (H_2O) are the three main hydrogen reservoirs in the stratosphere. Once an air parcel has entered the stratosphere, hydrogen can only be cycled between these reservoirs (as well as several short-lived species like OH, HO_2 or HCHO), since there are no net sources or sinks of hydrogen. Le Texier et al. [10] provide calculations of the relative amounts of H_2O and H_2, showing that the predominant production is that of water vapour in the vicinity of the stratopause. They indicate, however, that H_2 production in the mesosphere, and relatively strong descent in winter and early spring at high latitudes, may result in the upper stratosphere being relatively dry in these seasons and latitudes. Thus, the total hydrogen content $[H_2]=2[CH_4]+[H_2]+[H_2O]$, where [ ] denotes the mixing ratio, is generally constant in the stratosphere. The end product of CH_4 oxidation chains is H_2O. This means that changes in atmospheric mixing ratios of CH_4 has a potential impact on water vapor concentrations in the stratosphere. The chemical process of methane oxidation is believed to be reasonably well understood such that the complete oxidation of one methane molecule produces two water vapor molecules [11].

There is, nevertheless, good observational evidence that over much of the stratosphere the quantity $2[CH_4]+[H_2O]$ is quite uniformly distributed. The parametrization used the value 6 ppmv for the sum $2[CH_4]+[H_2O]$. This version was used in production of the ERA-40 re-analyses, which have been found to be generally drier in the stratosphere than the climatology derived by Randel et al.[12] from UARS measurements.

It is assumed that $2[CH_4]+[H_2O]=Q_{obs}$, where Q_{obs} is a value somewhat over 6 ppmv and it would be specially investigated according to numerous local observations.

We assume that the volume mixing ratio of water vapour $[H_2O]$ increases at a rate

$$\frac{dq_{ppmv}}{dt}=2k_1[CH_4] \tag{1}$$

We further assume that

$$2[CH_4]=Q_{obs}-[H_2O] \tag{2}$$

The rate of increase of volume mixing ratio of water vapour (in ppmv) is thus

$$\frac{dq_{ppmv}}{dt}=k_1(Q_{obs}-[H_2O]) \tag{3}$$

In terms of specific humidity, q, the source is

$$\frac{dq}{dt}=k_1(Q-q) \tag{4}$$

where (having divided by 1.6×10^6 to convert from volume mixing ratio in ppmv to specific humidity) the parameter Q has the value $Q=Q_{obs}/(1.6\times10^6)$ kg/kg.

The rate k_1 could be determined, for example, from a two-dimensional model with comprehensive chemistry, as in the scheme we prescribe a simple analytical form for k_1 which varies only with pressure.

The photochemical life time of water vapor is of the order of 100 days near the stratopause, 2,000 days at 10 hPa, and effectively infinite at the tropopause (Brasseur and Solomon, 1984) [13]. A prescription of k_1 that gives a reasonable profile up to the stratopause is provided by

$$k_1=\frac{1}{86400\tau_1} \tag{5}$$

where k_1 is given in s^{-1} and the timescale, τ_1, in days, is given in terms of pressure, p, in Pa, by

$$\tau_1=\begin{cases}100 & p\leqslant50\\ 100\left[1+\alpha_1\ln^4\left(\frac{p}{50}\right)\Big/\ln\left(\frac{10000}{p}\right)\right] & 50<p<10000\\ \infty & p\geqslant10000\end{cases} \tag{6}$$

where we define

$$\alpha_1=\frac{19\ln10}{\ln^4 20} \tag{7}$$

to give a time-scale of 2,000 days at the 10 hPa level.

This parametrization moistens rising air in the tropical stratosphere. This air will earlier have been freeze-dried near the tropopause, where specific humidity can locally fall well below 1 mg/kg. Specific humidity approaching the value Q will be reached near the stratopause. Descent near the poles will bring down air with specific humidity close to Q.

2.2 *Photolysis in the mesosphere*

For model versions with an upper most level at 0.1 hPa, or higher, it is necessary to include the sink of water vapor that occurs in the mesosphere and above due to photolysis. A simple representation of this effect is included, modifying the source term (4) by adding a decay term $-k_2q$ above a height of about 60 km. The full source/sink term becomes

$$k_1(Q-q)-k_2q \tag{8}$$

As for k_1, we take k_2 independent of latitude with parameters chosen to match the vertical profile of photochemical lifetime presented by Brasseur and Solomon (1984) [13]. Specifically,

$$k_2=\frac{1}{86400\tau_2} \tag{9}$$

$$\tau_2=\begin{cases}3 & p\leqslant 0.1\\ \left(\exp\left\{\alpha_2-0.5\left(\ln 100+\alpha_2\right)\left(1+\cos\dfrac{\pi\ln(p/20)}{\ln 0.005}\right)\right\}-0.01\right)^{-1} & 0.1<p<20\\ \infty & p\geqslant 20\end{cases} \tag{10}$$

$$\alpha_2=\ln\left(1/3+0.01\right) \tag{11}$$

3 DESIGN OF NUMERICAL SIMULATION

3.1 *Introduction of weather processes*

3.1.1 A HEAVY RAIN IN SOUTH CHINA

The heavy rain processes chosen for demonstration is a local rainstorm incident that occurred during 5-7 May 2010. The rainstorm is appearing ahead of the 500-hPa ridge. Surface shear, lower-vortex, front are favorable to the development of the rainstorm system.

The situation of upper trough, middle-lower shear and the south-west vortex moving eastward from Sichuan all contribute to the rainstorm system over South of the Changjiang River, South China, and east area of Southwest. The pumping action of upper-level divergence may be a trigger mechanism of this heavy rain. South China Sea is the main source of low level water vapor. Convergence and divergence of water vapor have an indicative meaning for development of rainstorm.

During 5-7 May 2010, the general precipitation of this process exceed 100 mm, and the main rainfall area located in the middle-east of Guangzhou and southwest of Fujian, which negatively affected traffic, agriculture and people's normal livelihood, and even caused the loss of properties and lives.

3.1.2 FITOW CAUSED STORM

Typhoon Fitow was the strongest typhoon to make landfall in Mainland China during October since 1949. The 21st named storm of the 2013 Pacific typhoon season, Fitow developed on September 29 to the east of the Philippines. It initially tracked north-northwestward, gradually intensifying into a tropical storm and later to typhoon status, or with winds of at least 120 km/h. Fitow later turned more to the west-northwest due to an intensifying ridge to the east, bringing the typhoon over the Ryukyu Islands with peak winds of 140 km/h on October 5. The next day, the typhoon struck China at Fuding in Fujian province, with a landfall pressure of 955 mbar according to the China Meteorological Administration (CMA). Fitow quickly weakened over land, dissipating on October 7.

After officially becoming a typhoon, Fitow turned more to the northwest due to the ridge building to the east. Despite increasing wind shear, the typhoon continued to intensify due to amplified outflow.

As Fitow made landfall in mainland China, it produced wind gusts of 274 km/h in the Shiping Mountains of Zhejiang, setting a record for the province. The typhoon spread heavy rainfall across eastern China in the Jiangnan region, in conjunction with a plume of cold air. An area 175,000 km^2 wide received 50 mm of precipitation, while an area of 38,000 km^2 wide received over 250 mm of rainfall. Yuyao in Zhejiang reported a peak rainfall total of 803 millimetres, a record for the city, while Ningbo reported a daily average of 390 mm over three days, setting a record. A station in Shanghai reported 152.9 mm, the highest daily rainfall total since 1961.

3.2 *Experimental configuration*

All numerical experiments are performed using the global spectral model of T799 with 25 km horizontal grid spacing and divides into 91 layers with different intervals in the vertical direction. The model top is at 0.01 hPa, or about 80 km. The integration time step is 90 s. The physics package includes parameterizations of radiative transfer, turbulent mixing, subgrid-scale orographic drag, moist convection, clouds and land surface processes.

Two cold-start runs with different parameterization configurations have been performed from 0000 UTC 05 May 2010. For the purpose of representing the impact of methane oxidation, control experiment and contrast experiment are carried using the above standard configuration, but respectively without and with the methane oxidation parameterization.

The same two cold-start runs with the same parameterization configurations have been performed from 0000 UTC 6 Oct 2013. These tests will focus on the impact of methane on the tropical water vapor distribution and on the Fitow caused tropical storm.

4 RESULTS AND ANALYSIS

Based on the analysis of this study, a simple conceptual model of the wind structure over complex mountainous topography under strong wind condition is shown in Fig.8.

4.1 *Results and analysis of heavy rain case*

Different simulating results of control experiment and contrast experiment of the 24 h accumulative precipitations from 0000UTC May 6 to 0000UTC May 7, 2010 are shown that the simulated results of distribution and tendency of rain belts, as well as the locations of rain centers of the two experiments are quite similar. The difference of the precipitation results of the two experiments is shown in Fig.1. It is obviously that the ranges of positive and negative values are distributed alternately. There is a negative center with value of -30 mm located in the south of Fujian, and a positive center with value of 20 mm located in the north of Yunnan. The simulating center value of contrast experiment is increased up to 10% than that of the control experiment. Simulating results indicated that

there is significant impact of methane oxidation parameterization on the precipitation.

Although the atmospheric methane concentration (hereafter AMC in mixing ratio) in the stratosphere is much less than that in the troposphere, methane is a very active component in photochemical processes in the stratosphere, where it influences the concentration of stratospheric water vapor and O_3, thereby influencing the stratospheric temperature. BI[14] concluded that Simulation results have shown that when the AMC is increased by 10%. The annual mean temperature will decrease by 0.2 K in the upper stratosphere, and the middle stratospheric cooling will exceed 0.05 K at mid- and high-latitudes.

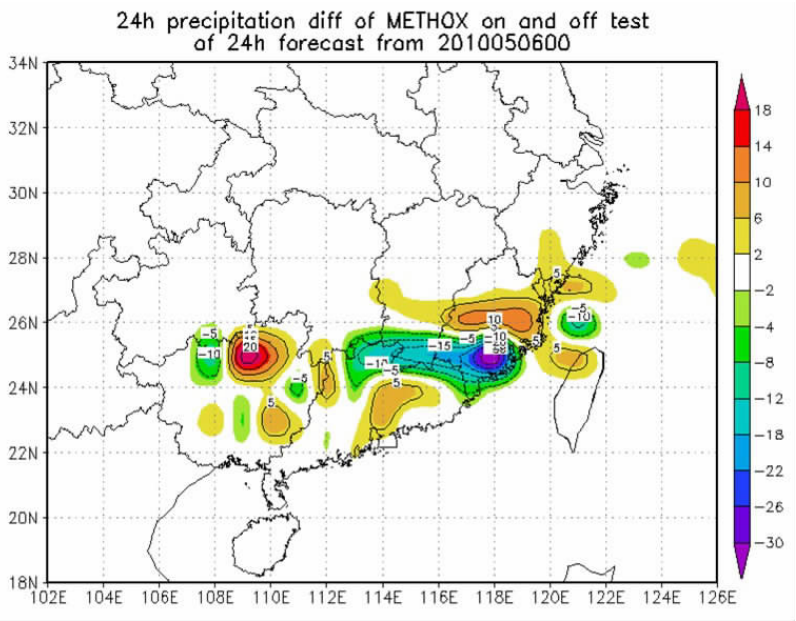

Figure 1. Difference of 24-h forecasting from 0000 UTC on 6 May 2010 of 24-h accumulative precipitation (unit: mm) in the south of China.

Figure 2 is the distribution of the difference of relative humidity and temperature at 100 hPa in the south of China. The shape and location of the ranges of positive and negative values of temperature is quite similar to that of the relative humidity, while the positive range of temperature difference is corresponding to the negative ranges of relative humidity difference, and vice versa.

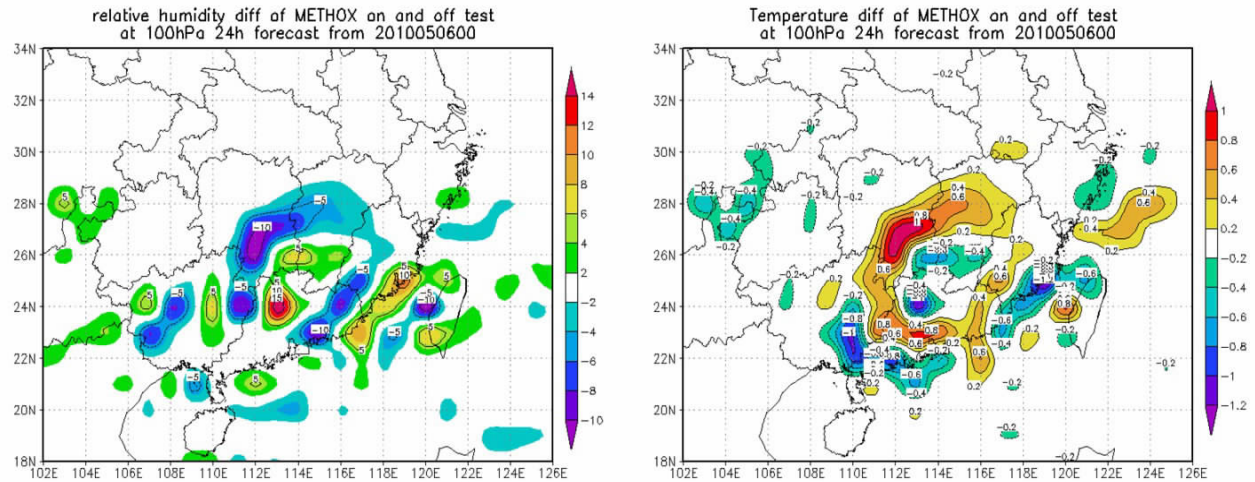

Figure 2. Difference of 24-h forecasting of relative humidity (unit: %) and temperature (unit: K) from 0000 UTC on 6 May 2010 at 100 hPa in the south of China.

For example, there is a negative center of relative humidity difference with value of 10% located in the central south of Hunan, where there is a positive center of temperature difference with value of 1K. It is suggested that the difference of relative humidity is relative to the difference of temperature, and there is a significant negative correlation between them.

Basing on the general knowledge that atmosphere

with more water vapor results in lower temperature, and higher temperature makes it contents less water vapor. The difference of temperature and relative humidity of control experiment and contrast experiment has negative correlation. It is illustrated that introduction of methane oxidation parametrization modified the distribution of water vapor and then producing a broadly realistic distribution of temperature.

However, the distribution of the difference of relative humidity and temperature at 100 hPa in the south of China presents is not obviously relative to that of the precipitation. It is indicated that the diagnostic precipitation is not directly affected by the change of the stratospheric water vapor and temperature, but primarily by the complex factors in the troposphere, such as the synoptic system and convection motion etc.

4.2 *Tropical humidity results and analysis*

Theoretically, values of water vapor in the tropical upper stratosphere, and throughout much of the extratropical stratosphere, would have been remedied by the introduction of parametrization of the upper-stratospheric moisture source due to methane oxidation. The actual efficiency of the methane oxidation parametrization and the influence degree of humidity field at different vertical layers in the stratosphere is concerned.

In order to indicate the capability of forecasting of moisture and temperature in stratosphere using the general circulation model with parametrization of methane oxidation, ERA-interim data is chose to verify the simulation of the distribution of global relative humidity to avoid the lack of observations in the stratosphere. Fig.3 displays the distribution of the global relative humidity at 100 hPa of ERA-interim data and simulating data. The simulating result is well reproduced the distribution of the global moisture field in stratosphere, and successfully describes the moist regions over tropical areas. While the simulating values of the relative humidity is quite smaller than those of the ERA-interim data.

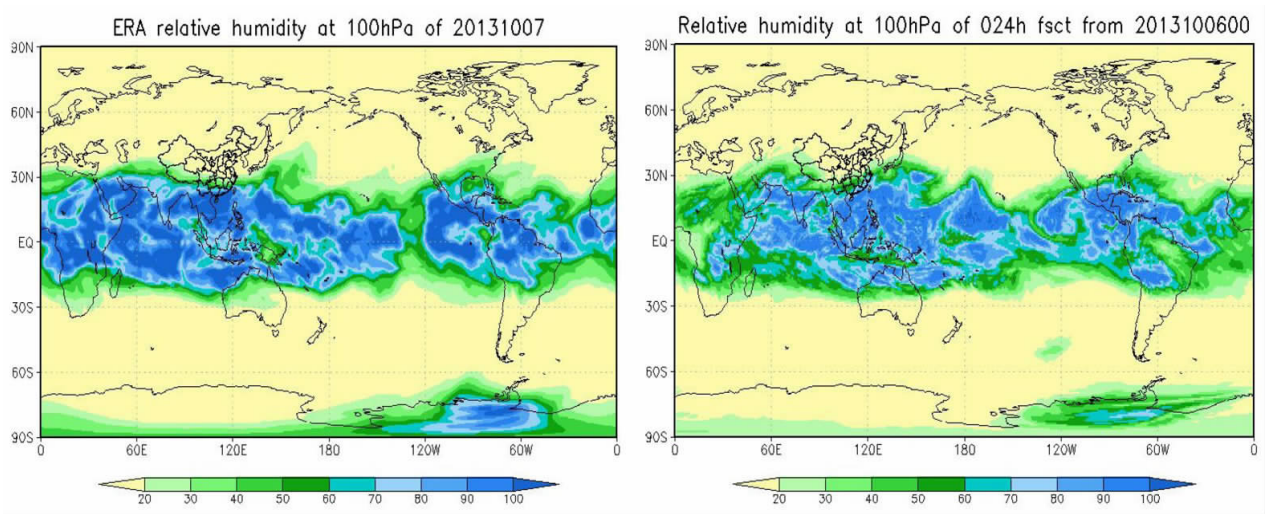

Figure 3. Global relative humidity (unit: %) at 100 hPa of ERA-interim data (left) on 7 October 2013 and 24-h forecasting (right) from 0000 UTC on 6 October 2013.

As shown in Fig.4, global difference of relative humidity at 50 hPa and 100 hPa of the two experiments is converged in the tropical upper stratosphere, and the difference value is beyond 25%. The detail difference of relative humidity at 100 hPa of the two experiments is presented in Fig.5 within local area. There is a dissymmetrical converge zone located between 20°S and 25°N, and the north edge of which even overruns 30°N. For China, it is apparent that the general impact of methane oxidation on the stratospheric humidity spreads throughout the wide south area of the Changjiang River. The results demonstrated that the deficiency has now been remedied by the introduction of a simple parametrization of the upper-stratospheric moisture source due to methane oxidation. Different sensitivity of parametrization of methane oxidation is corresponding to the different vertical layers.

Methane reaches the stratosphere and mesosphere from the troposphere through vertical motion. The vertical gradient of the methane volume mixing ratio is very small in the troposphere, but the ratio quickly decreases with altitude in the middle atmosphere because methane is very active chemically, meaning it is ultimately destroyed by a series of reactions within the stratosphere [13].

4.3 *Tropical temperature results and analysis*

Methane acts as the primary source of in situ hydration of the stratosphere via a sequence of reactions which lead to the formation of both formaldehyde and molecular hydrogen. Both of these species can be oxidized in the stratosphere resulting in net gain of water vapor. The effect of these reactions varies somewhat with latitude, height, and season due to the interaction of dynamical processes and the competition

between chemical reactions. Because of its activity in photochemical processes, stratospheric methane influences the concentration of stratospheric water vapor and O_3, and obviously influences the radiation process in the stratosphere, finally influencing the stratospheric temperature.

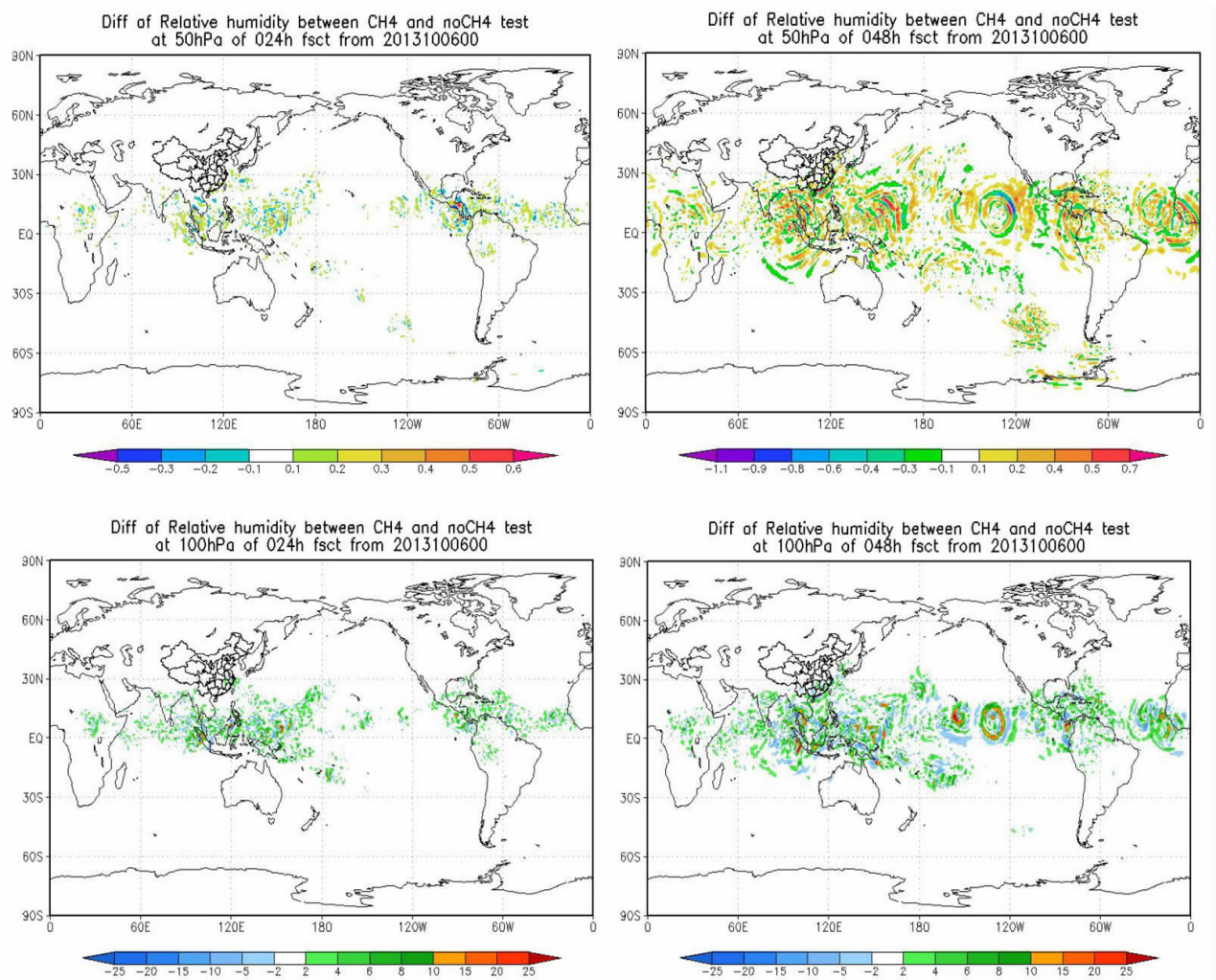

Figure 4. Global difference of 50 hPa(up) and 100 hPa(down) relative humidity(unit:%) of 24 h(left) and 48h(right) forecasting from 0000UTC at 6 October 2013.

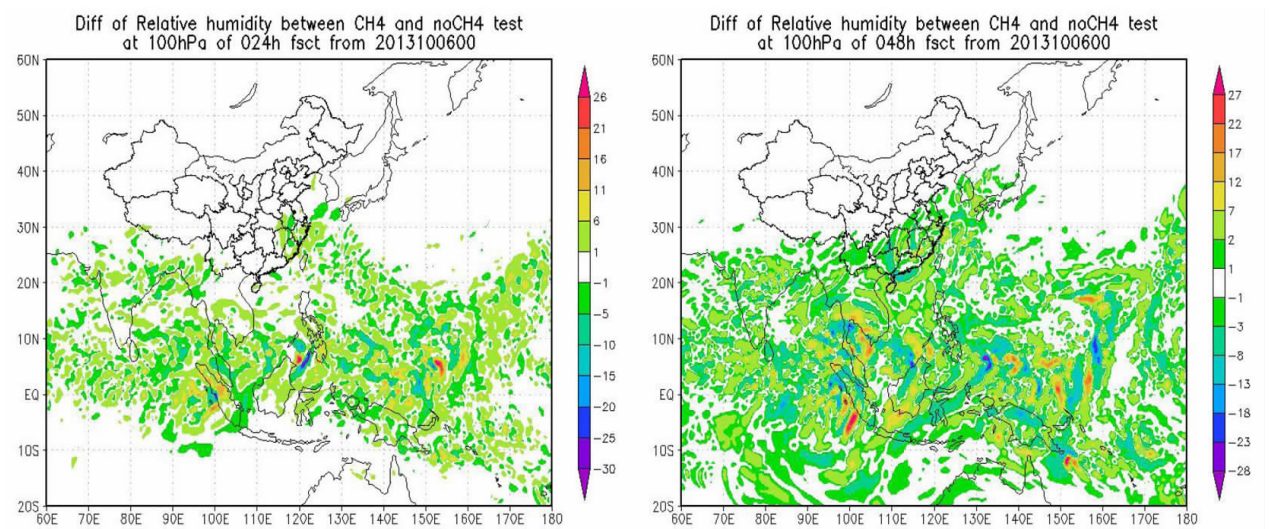

Figure 5. Local difference of 100-hPa relative humidity (unit: %) of 24 h (left) and 48 h (right) forecasting from 0000 UTC on 6 October 2013 of relative humidity.

As shown in Fig.6, global difference of temperature at 50 hPa and 100 hPa of the two experiments is mainly distributed in the low stratosphere over the tropical and Pacific areas, and the difference value is up to 1.5 K at 50 hPa and 3.2 K at 100 hPa. The 168-h forecasting difference of relative humidity at 50 hPa and 100 hPa of the two experiments is presented in Fig.7. There is a converge zone located between 30°S and 30°N, and the maximal difference value of relative humidity is 3.3% at 50 hPa and even 30% at 100 hPa. It is noticeable that there is an obvious eddy over the north to Philippines and where is near to the Typhoon Lily located on 13 Oct. While the 168 h forecasting difference of temperature is shown in Fig.8, which not converges over the tropical but spreads throughout the world, and the eddy over north to Philippines is still presented.

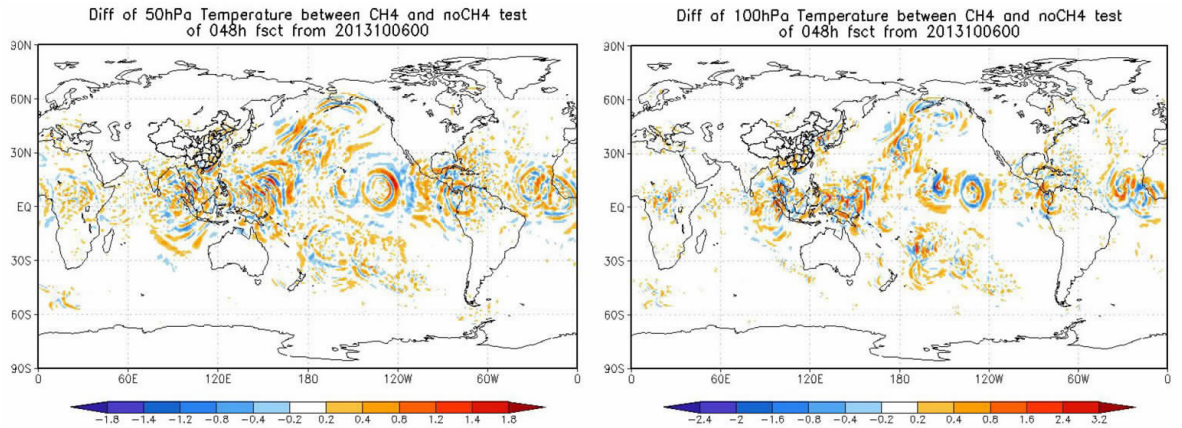

Figure 6. Global difference of 50 hPa(left) and 100 hPa(right) temperature(unit:K) of 48h forecasting from 0000 UTC at 6 Oct 2013.

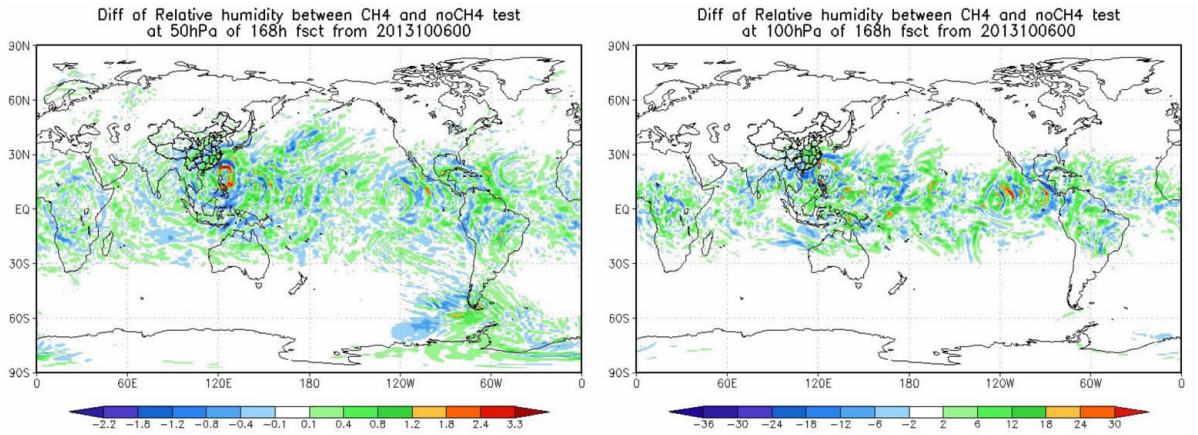

Figure 7. Global difference of 50 hPa (left) and 100 hPa (right) relative humidity (unit: %) of 168 h forecasting from 0000 UTC at 6 Oct 2013.

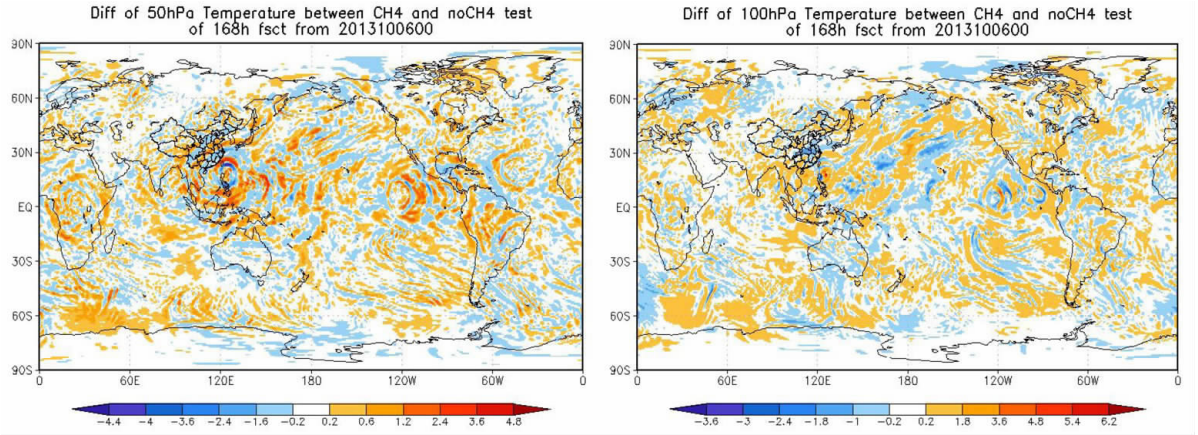

Figure 8. Global difference of 50 hPa (left) and 100 hPa (right) temperature (unit: K) of 168 h forecasting from 0000 UTC at 6 Oct 2013.

4.4 *Forecast verification*

To have an idea about the impact of methane oxidation parameterization schemes on the forecast quality, two different forecasts for 40 days started from two 4D-Var assimilations using same observations and back-ground fields, but separately with and without methane parameterization were conducted.

Objective weather forecast verification can be performed from at least three different perspectives: accuracy (the difference between forecast and verification), skill (comparison with some reference method, such as persistence, climate or an alternative forecast system) They are all "objective" in the sense that the numerical results are independent of who calculated them, but not necessarily objective with respect to what is considered "good" or "bad".

The most common accuracy measure is the Root Mean Square Error (RMSE). The RMSE of forecasts (F) relative to analyses (Av) can be defined as

$$\mathrm{RMSE}=\left[\frac{1}{N}\sum (F-A)^2\right]^{\frac{1}{2}} \quad (12)$$

which measures the distance between the forecast and the verifying analysis. The RMSE is negatively orientated, i.e. increasing numerical values indicate increasing "failure".

The forecast performance of 240 h high-resolution forecast with and without methane parameterization of Dec 2013 over the tropics, as measured by monthly mean of root mean square (RMS) errors of the geopotential height, temperature and winds at 500 hPa forecast with respect to the analysis, is shown in Table 1. The slightly decrease in error of temperature and winds in most days is associated with the introduction of methane parameterization. The error of geopotential height is decreased at the 5-day range and increased during 8-10 days.

Table 1. Monthly mean of root mean square (RMS) error over the tropics (20°S-20°N) between 240-h forecast and verifying analysis of 500-hPa geopotential height, temperature and winds of noch4 and ch4 test during December 2013.

RMS	Test	forecast range (in days)									
		1	2	3	4	5	6	7	8	9	10
Height	noch4	4.147	5.593	6.404	7.844	9.346	10.808	12.258	13.296	14.077	14.767
(pgm)	ch4	4.143	5.593	6.407	7.822	9.308	10.840	12.246	13.352	14.182	14.867
Temp.	noch4	0.403	0.541	0.643	0.726	0.819	0.896	0.971	1.070	1.145	1.214
(K)	ch4	0.400	0.538	0.643	0.726	0.815	0.896	0.971	1.057	1.132	1.214
Wind	noch4	2.993	4.341	5.318	6.107	6.777	7.324	7.787	8.339	8.868	9.419
(m/s)	ch4	2.987	4.338	5.300	6.115	6.781	7.324	7.779	8.300	8.859	9.419

Another way to measure the quality of a forecast system is to calculate the correlation between forecasts and observations. However, correlating forecasts directly with observations or analyses may give misleadingly high values because of the seasonal variations. It is therefore established practice to subtract the climate average from both the forecast and the verification and to verify the forecast and observed ***anomalies*** according to the anomaly correlation coefficient (ACC), which in its most simple form can be written:

$$\mathrm{ACC}=\frac{\sum (F-C-M_{fc})(Av-C-M_{vc})}{\left[\sum (F-C-M_{fc})^2 \sum (Av-C-M_{vc})^2\right]^{\frac{1}{2}}} \quad (13)$$

$$M_{fc}=\frac{1}{N}\sum (F-C),\ M_{vc}=\frac{1}{N}\sum (A_v-C) \quad (14)$$

The ACC can be regarded as a ***skill score relative to the climate***. It is positively orientated, with increasing numerical values indicating increasing "success". It has been found empirically that ACC=60% corresponds to the range up to which there is synoptic skill for the largest scale weather patterns.

Table 2 shows the forecast results of Dec 2013 in terms of monthly mean anomaly correlation (ACC) over the tropics of 500-hPa geopotential height, temperature and winds. The tropical scores have been consistently very good of the 240-h forecast with and without the introduction of methane parameterization, remaining above 80% up to day 7. The skill score of 240-h temperature forecast of ch4 test is a bit higher than noch4 test at day 1, day 5, day 8 and day 9, and equal at other days. It indicates that impact of methane parameterization in tropics is slightly positive as to the temperature, while it is neutral as to geopotential height and winds.

It is concluded that the impact of the including a stratospheric moisture source due to methane oxidation and a sink due to photolysis in the mesosphere is neutral as to the forecasting of geopotential height, and positive to the forecasting of temperature and winds over the tropics.

5 CONCLUSIONS AND DISCUSSION

This study presents the advantages of methane oxidation parametrization in producing a realistic distribution of water vapor in the tropical stratosphere and analyzes the impact of methane chemical process on the general circulation model using two heavy rain cases. It is obvious that general circulation model with

Table 2. Monthly mean of anomaly correlation (ACC) over the tropics (20°S-20°N) between 240-h forecast and verifying analysis of 500-hPa geopotential height, temperature and winds of noch4 and ch4 test during December 2013.

ACC	Test	forecast range (in days)									
		1	2	3	4	5	6	7	8	9	10
Height	noch4	0.970	0.949	0.941	0.914	0.883	0.841	0.804	0.774	0.751	0.728
	ch4	0.971	0.949	0.940	0.914	0.884	0.840	0.805	0.773	0.748	0.725
Temp.	noch4	0.929	0.877	0.834	0.786	0.734	0.688	0.632	0.580	0.520	0.482
	ch4	0.930	0.877	0.834	0.786	0.736	0.688	0.632	0.584	0.523	0.481
Wind	noch4	0.938	0.884	0.825	0.761	0.689	0.613	0.537	0.472	0.414	0.363
	ch4	0.938	0.885	0.826	0.760	0.690	0.613	0.537	0.471	0.409	0.364

methane oxidation parametrization succeeds in simulating the water vapor and temperature in stratosphere. Objective weather forecast verifications have been performed using simulating results of one month, which demonstrate somewhat positive effects on the model skill. The following conclusions can be drawn:

(1) There is a certain extent impact of methane oxidation parameterization on the precipitation. The simulating rain center value of contrast experiment is increased up to 10% than that of the control experiment.

(2) There is significant efficiency of the methane oxidation parametrization, and the influence degree of humidity field is obvious in the lower stratosphere such as the 100-hPa and 50-hPa layers.

(3) Introduction of methane oxidation parametrization has modified the distribution of water vapor and then producing a broadly realistic distribution of temperature.

(4) The verification of monthly mean of forecast anomaly correlation (ACC) and root mean square (RMS) errors over the tropics indicates that the impact of stratospheric methane is neutral as to the forecast of 500 hPa geopotential height, and positive to the forecast of temperature and winds over the tropics.

It is prospected that the introduction of a simple methane oxidation parametrization into the general circulation model will be of benefit to describing the stratospheric characters and thus improving the prediction of both stratosphere and troposphere.

As one of the most important greenhouse gas, methane can change the radiation effect in the stratosphere by absorbing the longwave radiation. A globally averaged value for CH_4 by bi-dimensional (latitude/height) climatological fields derived from the MOBIDIC model is used in the currently general circulation model. Xie et al. [15] investigated the contribution of the radiative heating effect of increasing CH_4 on the tropopause to the stratospheric water vapor increases. As a part of the future work，more numerical experiments and further research with regard to interaction of radiation and methane should be carried out.

In the longer term, in order to improve the representation of stratospheric water vapor, increased vertical resolution near the tropical tropopause and refinements in parametrization, especially in respect of deep convection, stratiform cloud processes and radiation would be investigated.

REFERENCES:

[1] ZHENG Bin, SHI Chun-hua, CHEN Yue-Juan. Distribution features and seasonal variations of stratospheric CH_4 over China [J]. J Altiplano Meteorol, 2006, 25(4): 609-615.

[2] BI Yun, CHEN Yue-juan, XU Li, et al. Analysis of H_2O and CH_4 distribution characteristics in the middle atmosphere using HALOE data [J]. Chin J Atmos Sci, 2007, 31(3): 440-448.

[3] GUO Shi-chang, ZHOU Hong, LV Da-ren, et al. Temporal and spatial features of atmospheric methane and its relation to ozone variation in the stratosphere [J]. J Yunnan Univ, 2008, 30(4): 381-387.

[4] ZHENG Bin, SHI Chun-hua. An Influence Of Quqsi-Biennial Osciliation On The Double Peaks Of CH_4 In The Sratosphere [J]. J Trop Meteorol, 2008, 24(2): 111-116.

[5] BI Yun, CHEN Yue-juan, ZHOU Ren-jun, et al. Interannual change of extra-tropical methane induced by the quasi-biennial oscillation of tropical wind and its formation mechanism [J]. J Trop Meteorol, 2011, 17(4): 375-384.

[6] BLAKE D R, ROWLAND F S. Continuing worldwide increase in tropospheric methane, 1978-1987 [J]. Science, 1988, 239, 1129-1131.

[7] DLUGOKENCKY E J, Walter B P, Masarie K A, et al. Measurements of an anomalous global methane increase during 1998 [J]. Geophys Res Lett, 2001, 28, 499-502.

[8] ENGEL A, Schiller C, Schmidt U, et al. The total hydrogen budget in the Arctic winter stratosphere during the European Arctic Stratospheric Ozone Experiment [J]. J Geophys Res, 1996, 101(14): 495-504.

[9] SIMMONS A J, Untch A, Jacob C, et al. Stratospheric water vapour and tropical tropopause temperatures in ECMWF analyses and muli-year simularions [J]. Quart J Roy Meteorol Soc, 1999, 125, 353-386.

[10] Le TEXIER L, SOLOMON S, GARCIA R R. The role of molecular hydrogen and methane oxidation in the water vapour budget of the stratosphere [J]. Quart J Roy Meteorol Soc, 1988, 114: 281-295.

[11] BRASSEUR G, SOLOMON S. Aeronomy of the Middle Atmosphere [M]. 3rd ed, Springer, Dordrecht, Netherlands, 2005.

[12] RANDEL W J, WU F, RUSSELL J M, et al. Seasonal cycles and QBO variations in straospheric CH_4 and H_2O observed in UARS HALOE data [J]. J Atmos Sci, 1998, 55: 163-185.
[13] BRASSEUR G, SOLOMON S. Aeronomy of the Middle Atmosphere [M]. D. Reidel Publishing Co. 1984.
[14] BI Yun, CHEN Yue-juan, ZHOU Ren-jun, et al. Simulation of the effect of an increase in methane on air temperature [J]. Adv Atmos Sci, 2011, 28(1): 129-138.
[15] XIE Fei, TIAN Wen-shou, LI Jian-ping, et al. The possible effets of future increase in methane emission on the stratospheric water vapor and global ozone [J]. Acta Meteorol Sinica, 2013, 71(3): 555-567.

Citation: WANG Shu-chang, ZHAO Jun, WU Jian-ping et al. Numerical simulation of influence of stratospheric methane on tropical water vapor and temperature [J]. J Trop Meteorol, 2017, 23(1): 103-112.